

Tensor Ring Decomposition with Rank Minimization on Latent Space: An Efficient Approach for Tensor Completion

Anonymous Authors

Affiliation

Address

email

Abstract

In tensor completion tasks, the traditional low-rank tensor decomposition models suffer from laborious model selection problem due to high model sensitivity. Especially for tensor ring (TR) decomposition, the number of model possibility grows exponentially with the tensor order, which makes it rather challenging to find the optimal TR decomposition. In this paper, by exploiting the low-rank structure on TR latent space, we propose a novel tensor completion method, which is robust to model selection. In contrast to imposing low-rank constraint on the data space, we introduce nuclear norm regularization on the latent TR factors, resulting in that the optimization step using singular value decomposition (SVD) can be performed at a much smaller scale. By leveraging the alternating direction method of multipliers (ADMM) scheme, the latent TR factors with optimal rank and the recovered tensor can be obtained simultaneously. Our proposed algorithm effectively alleviates the burden of TR-rank selection, therefore the computational cost is greatly reduced. The extensive experimental results on synthetic data and real-world data demonstrate the superior high performance and efficiency of the proposed approach against the state-of-the-art algorithms.

Introduction

Tensor decomposition aims to find the latent factors of tensor-valued data (i.e. the generalization of multi-dimensional arrays), thereby casting large-scale tensors into a multilinear tensor latent space of low-dimensionality (very few degrees of freedom designated by the rank). The latent factors of tensor decomposition can be considered as the latent features of data, thus they can be used to predict missing entries when the acquired data is incomplete. The specific forms and operations among latent factors determine the type of tensor decomposition. The most classical and successful tensor decomposition models are Tucker decomposition and CANDECOMP/PARAFAC (CP) decomposition (Kolda and Bader 2009), after which the matrix product state/tensor-train (MPS/TT) has drawn people's attention owing to its super compression and computational efficiency properties (Oseledets 2011). Furthermore, in recent years, a generalization of TT decomposition, termed the tensor ring (TR) decomposition, is studied across disciplines (Zhao et al. 2016a; Zhao et al. 2018). These tensor

decomposition models have been applied in various fields such as machine learning (Novikov et al. 2015; Anandkumar et al. 2014; Kanagawa et al. 2016), signal processing (Cong et al. 2015), image/video completion (Liu et al. 2013; Zhao et al. 2016b), compressed sensing (Gandy, Recht, and Yamada 2011), to name but a few.

Tensor completion is one of the most popular applications for tensor decomposition, which is to recover the incomplete tensor from partially observed entries. The theoretical lynchpin in tensor completion problems is the tensor low-rank assumption. Many tensor low-rank approximation methods are proposed for tensor completion and the tensor completion methods can mainly be categorized into two types: tensor decomposition based approach and rank minimization based approach. Tensor decomposition based methods find tensor latent factors by the incomplete tensor, then the latent factors are used to predict the missing entries. Based on alternating least squares (ALS) method (Grasedyck, Kluge, and Kramer 2015; Wang, Aggarwal, and Aeron 2017), gradient-based method (Yuan, Zhao, and Cao 2017; Acar et al. 2011), etc, many completion algorithms have been proposed. Though ALS and gradient-based algorithms are free from burdensome hyper-parameter tuning work, the performance of these algorithms is rather sensitive to model selection, i.e., rank selection of the tensor decomposition. Moreover, since the optimal rank in the model is generally data-dependent, it is very challenging to specify the optimal rank beforehand. Especially for Tucker, TT, and TR, of which the rank is defined as a vector, it is impossible to find the optimal ranks by cross-validation method due to immense rank selection possibilities. The other type of tensor completion method is based on rank minimization which employs convex surrogates to minimize the tensor rank. One of the most commonly used surrogates is the nuclear norm (a.k.a. Schatten norm, or trace norm), which is defined as the sum of singular values of a matrix and it is the most popular convex surrogate for rank regularization. Based on different definition of tensor rank, various nuclear norm regularized algorithms are proposed (Liu et al. 2013; Imaizumi, Maehara, and Hayashi 2017; Liu et al. 2014; Liu et al. 2015). The rank minimization based methods do not need to specify the rank of decompositions beforehand, and the rank of the recovered tensor will be automatically learned from the limited observations. However, these algo-

gorithms face multiple large-scale SVD operations on the unfoldings of the tensor when employing the nuclear norm and numerous hyper-parameters tuning problems, which lead to high computational cost and low efficiency.

To address the problems of high sensitivity to rank selection and low computational efficiency in traditional tensor completion methods, in this paper, we propose a new algorithm named tensor ring low-rank factors (TRLRF) which effectively alleviates the burden of rank selection and reduce the computational cost. We take a virtue of applying both the nuclear norm regularization and the tensor decomposition to our model, thus providing model performance stability and high computational efficiency. The proposed method is efficiently solved by ADMM algorithm and it simultaneously achieves tensor decomposition and completion based on TR decomposition. Our main contributions of this paper are listed below:

- We theoretically reveal the relationship between the multilinear tensor rank and the rank of TR factors, under which the low-rank constraint can be performed implicitly on TR latent space. This leads to fast SVD calculation on small size factors.
- The nuclear norm is further imposed to regularize the TR-ranks, by which our algorithm can always obtain the stable solution, even if the TR-rank is misspecified. This indicates our model is of rank-robustness.
- We develop an efficient algorithm based on ADMM to optimize the proposed model, by which the TR-factors and the recovered tensor are obtained simultaneously.

In addition, the results of extensive experiments on synthetic data and real-world data show that our TRLRF outperforms the state-of-the-art algorithms. Furthermore, the experimental results also illustrate that our proposed algorithm is robust to model selection and can be applied to high-order tensors, resulting in low computational cost.

Preliminaries and Related Works

Notations

The notations in (Kolda and Bader 2009) are adopted in this paper. A scalar is denoted by a normal lowercase letter or a uppercase letter, e.g., $x, X \in \mathbb{R}$, and a vector is denoted by a boldface lowercase letter, e.g., $\mathbf{x} \in \mathbb{R}^I$. A matrix is denoted by a boldface capital letter, e.g., $\mathbf{X} \in \mathbb{R}^{I \times J}$. A tensor of order $N \geq 3$ is denoted by calligraphic letters, e.g., $\mathcal{X} \in \mathbb{R}^{I_1 \times I_2 \times \dots \times I_N}$. $\{\mathcal{X}^{(n)}\}_{n=1}^N := \{\mathcal{X}^{(1)}, \mathcal{X}^{(2)}, \dots, \mathcal{X}^{(N)}\}$ is defined as a tensor sequence, where $\mathcal{X}^{(n)}$ denotes the n -th tensor of the sequence. The sequence can also be simply written as $[\mathcal{X}]$ if there is no confusion. The representations of matrix sequences and vector sequences are denoted in the same way. An element of tensor $\mathcal{X} \in \mathbb{R}^{I_1 \times I_2 \times \dots \times I_N}$ of index (i_1, i_2, \dots, i_N) is denoted by $\mathcal{X}(i_1, i_2, \dots, i_N)$ or $x_{i_1 i_2 \dots i_N}$. The inner product of two tensors \mathcal{X}, \mathcal{Y} with the same size $\mathbb{R}^{I_1 \times I_2 \times \dots \times I_N}$ is defined as $\langle \mathcal{X}, \mathcal{Y} \rangle = \sum_{i_1} \sum_{i_2} \dots \sum_{i_N} x_{i_1 i_2 \dots i_N} y_{i_1 i_2 \dots i_N}$. Furthermore, the Frobenius norm of \mathcal{X} is defined by $\|\mathcal{X}\|_F = \sqrt{\langle \mathcal{X}, \mathcal{X} \rangle}$.

We employ two types of tensor unfolding (matricization) operations in this paper. The one mode- n unfolding (Kolda and Bader 2009) of tensor $\mathcal{X} \in \mathbb{R}^{I_1 \times I_2 \times \dots \times I_N}$ is denoted by $\mathbf{X}_{(n)} \in \mathbb{R}^{I_n \times I_1 \dots I_{n-1} I_{n+1} \dots I_N}$. Moreover, another mode- n unfolding of tensor \mathcal{X} which is often used in TR operations (Zhao et al. 2016a) is denoted by $\mathbf{X}_{\langle n \rangle} \in \mathbb{R}^{I_n \times I_{n+1} \dots I_N I_1 \dots I_{n-1}}$. Furthermore, the inverse operation of unfolding is matrix folding (tensorization), which transforms matrices to higher-order tensors. In this paper, we only define the folding operation for the first mode- n unfolding as $\text{fold}_n(\cdot)$, i.e., for a tensor \mathcal{X} , we have $\text{fold}_n(\mathbf{X}_{(n)}) = \mathcal{X}$.

Tensor ring decomposition

Tensor ring (TR) decomposition is a more general decomposition model than tensor-train (TT) decomposition. It represents a tensor with high-order by circular multilinear products over a sequence of low-order latent core tensors, i.e., TR factors. For $n = 1, \dots, N$, the TR factors are denoted by $\mathcal{G}^{(n)} \in \mathbb{R}^{R_n \times I_n \times R_{n+1}}$ and each consists of two rank-modes (i.e. mode-1 and mode-3) and one dimension-mode (i.e. mode-2). The syntax $\{R_1, R_2, \dots, R_N\}$ denotes the TR-rank which controls the model complexity of TR decomposition. TR decomposition applies trace operations and all of the TR factors are set to be order-three equivalently, thus TR decomposition relaxes the rank constraint on the first and last core of TT to $R_1 = R_{N+1}$. Moreover, TR decomposition linearly scales to the order of the tensor, thus it can overcome the ‘curse of dimensionality’. In this case, TR can be considered as a linear combination of TT and thus offers a powerful and generalized representation ability. The element-wise relation of TR decomposition and the generated tensor is given by equation (1):

$$\mathcal{X}(i_1, i_2, \dots, i_N) = \text{Trace} \left\{ \prod_{n=1}^N \mathbf{G}_{i_n}^{(n)} \right\}, \quad (1)$$

where $\text{Trace}\{\cdot\}$ is the matrix trace operation, $\mathbf{G}_{i_n}^{(n)} \in \mathbb{R}^{R_n \times R_{n+1}}$ is the i_n -th mode-2 slice matrix of $\mathcal{G}^{(n)}$, which also can be denoted by $\mathcal{G}^{(n)}(:, i_n, :)$ according to Matlab operation.

Tensor completion

Completion by TR decomposition Tensor decomposition based algorithms do not directly employ the rank constraint to the object tensor. Instead, they try to find the low-rank representation (i.e. tensor decompositions) of the incomplete data by observed entries. The obtained latent factors of the tensor decomposition are used to predict the missing entries. For model formulation, the tensor completion problem is set as a weighted least squares model. Based on different tensor decompositions, various tensor completion algorithms have been proposed, e.g., weighted CP (Acar et al. 2011), weighted Tucker (Filipović and Jukić 2015), TR-WOPT (Yuan, Zhao, and Cao 2017) and TRALS (Wang, Aggarwal, and Aeron 2017). To the best of our knowledge, there are two proposed TR-based tensor completion algorithm: TRALS and TRWOPT. They apply the same opti-

mization model and it is formulated as:

$$\min_{[\mathcal{G}]} \|P_{\Omega}(\mathcal{T} - \Psi([\mathcal{G}]))\|_F^2, \quad (2)$$

of which the optimization object is the TR factors $[\mathcal{G}]$. $P_{\Omega}(\mathcal{T})$ denotes all the observed entries w.r.t. the set of indices of observed entries represented by Ω , and $\Psi([\mathcal{G}])$ denotes the approximated tensor generated by $[\mathcal{G}]$. Every element of $\Psi([\mathcal{G}])$ is calculated by equation (1). The two algorithms are both based on the model (2). However, TRALS applies alternative least squares (ALS) method and TRWOPT uses gradient-based algorithm to solve the model, respectively. They perform well in both low-order and high-order tensors due to the high representative ability and flexibility of TR decomposition. However, these algorithms are shown to suffer from high sensitiveness to rank selection, which would lead to high computational cost.

Completion by nuclear norm regularization The model of rank minimization-based tensor completion can be formulated as:

$$\min_{\mathcal{X}} \text{Rank}(\mathcal{X}) + \frac{\lambda}{2} \|P_{\Omega}(\mathcal{T} - \mathcal{X})\|_F^2, \quad (3)$$

where \mathcal{X} is the recovered low-rank tensor, and $\text{Rank}(\cdot)$ is a rank regularizer. The model can find the low-rank structure of the data and approximate the recovered tensor. Because determining the tensor rank is an NP-hard problem (Hillar and Lim 2013; Kolda and Bader 2009), work in (Liu et al. 2013) and (Signoretto et al. 2014) extends the concept of low-rank matrix completion and defines the tensor rank as the sum of the rank of mode- n unfolding of the object tensor. Moreover, the convex surrogate named nuclear norm is applied for tensor low-rank model and it simultaneously regularizes all the mode- n unfoldings of the object tensor. In this way, model (3) can be reformulated as:

$$\min_{\mathcal{X}} \sum_{n=1}^N \|\mathbf{X}_{(n)}\|_* + \frac{\lambda}{2} \|P_{\Omega}(\mathcal{T} - \mathcal{X})\|_F^2, \quad (4)$$

where $\|\cdot\|_*$ denotes the nuclear norm regularization which is the sum of the singular values of the matrix. Usually the model is solved by ADMM algorithms and it is shown to have fast convergence and good performance when data size is small. However, when we need to deal with large-scale data, the multiple SVD operations in the optimization step will be intractable due to high computational cost.

Tensor Ring Low-rank Factors

Traditional rank minimization based tensor completion methods give nuclear norm regularization on multiple matrices generated by tensor unfoldings, they suffer from high computational cost of large-scale SVD operations in every iteration. To solve this problem, we give low-rankness on each of the TR factors and our basic tensor completion model is formulated as follow:

$$\begin{aligned} \min_{[\mathcal{G}], \mathcal{X}} \sum_{n=1}^N \|\mathcal{G}^{(n)}\|_* + \frac{\lambda}{2} \|\mathcal{X} - \Psi([\mathcal{G}])\|_F^2, \\ \text{s.t. } P_{\Omega}(\mathcal{X}) = P_{\Omega}(\mathcal{T}). \end{aligned} \quad (5)$$

We need firstly to deduce the relation of the tensor rank and the corresponding core tensor rank, which can be explained by the following theorem:

Theorem 1. Given an N -th order tensor $\mathcal{X} \in \mathbb{R}^{I_1 \times I_2 \times \dots \times I_N}$ which can be represented by equation (1), then the following inequality holds for all $n = 1, \dots, N$:

$$\text{Rank}(\mathbf{G}_{(2)}^{(n)}) \geq \text{Rank}(\mathbf{X}_{(n)}). \quad (6)$$

Proof. For the n -th core tensor $\mathcal{G}^{(n)}$, according to the works in (Zhao et al. 2016a), we have:

$$\mathbf{X}_{\langle n \rangle} = \mathbf{G}_{(2)}^{(n)} (\mathbf{G}_{\langle 2 \rangle}^{(\neq n)})^T, \quad (7)$$

where $\mathcal{G}^{(\neq n)} \in \mathbb{R}^{R_{n+1} \times \dots \times R_N}$ is a subchain tensor by merging all but the n -th core tensor. Hence, the relation of the rank satisfies:

$$\begin{aligned} \text{Rank}(\mathbf{X}_{\langle n \rangle}) &\leq \min\{\text{Rank}(\mathbf{G}_{(2)}^{(n)}), \text{Rank}(\mathbf{G}_{\langle 2 \rangle}^{(\neq n)})\} \\ &\leq \text{Rank}(\mathbf{G}_{(2)}^{(n)}). \end{aligned} \quad (8)$$

The proof is completed by:

$$\text{Rank}(\mathbf{X}_{\langle n \rangle}) = \text{Rank}(\mathbf{X}_{(n)}) \leq \text{Rank}(\mathbf{G}_{(2)}^{(n)}), \quad (9)$$

□

The theorem proves the relation between the tensor rank and the rank of the TR factors. The rank of mode- n unfolding of the tensor \mathcal{X} is upper bounded by the rank of the dimension-mode unfolding of the corresponding core tensor $\mathcal{G}^{(n)}$, thus we can give low-rank constraint on $\mathcal{G}^{(n)}$. By the new surrogate, our model (5) is reformulated by:

$$\begin{aligned} \min_{[\mathcal{G}], \mathcal{X}} \sum_{n=1}^N \|\mathbf{G}_{(2)}^{(n)}\|_* + \frac{\lambda}{2} \|\mathcal{X} - \Psi([\mathcal{G}])\|_F^2 \\ \text{s.t. } P_{\Omega}(\mathcal{X}) = P_{\Omega}(\mathcal{T}). \end{aligned} \quad (10)$$

The above model imposes nuclear norm regularization on the dimension-mode unfoldings of the TR factors, which can largely decrease the computational complexity compared to the algorithms which are based on model (4). Moreover, we consider to give low-rank constraints on the two rank-modes of the TR factors, i.e., the unfoldings of the TR factors along mode-1 and mode-3, which can be expressed by $\sum_{n=1}^N \|\mathbf{G}_{(1)}^{(n)}\|_* + \sum_{n=1}^N \|\mathbf{G}_{(3)}^{(n)}\|_*$. When the model is optimized, nuclear norms of the rank-mode unfoldings and the fitting error of the approximated tensor are minimized simultaneously, resulting in the initial TR-rank becomes the upper bound of the real TR-rank of the tensor, thus giving the ability of rank selection robustness to our model. The tensor ring low-rank factors (TRLRF) model is finally expressed by:

$$\begin{aligned} \min_{[\mathcal{G}], \mathcal{X}} \sum_{n=1}^N \sum_{i=1}^3 \|\mathbf{G}_{(i)}^{(n)}\|_* + \frac{\lambda}{2} \|\mathcal{X} - \Psi([\mathcal{G}])\|_F^2 \\ \text{s.t. } P_{\Omega}(\mathcal{X}) = P_{\Omega}(\mathcal{T}). \end{aligned} \quad (11)$$

Our TRLRF model has two distinctive advantages. Firstly, the low-rank assumption is placed on tensor factors instead

of on the original tensor, this reduces the computational complexity of the SVD operation largely. Secondly, low-rankness on tensor factors can enhance the robustness to rank selection, which can alleviate the burden of searching for optimal TR-rank and reduce the computational cost in the experiment.

Solving scheme

To solve model (11), we apply the alternating direction method of multipliers (ADMM) which is efficient and widely used (Boyd et al. 2011). Moreover, because the variables of TRLRF model are inter-dependent, we impose auxiliary variables to simplify the optimization. Thus the TRLRF model is rewritten as:

$$\begin{aligned} \min_{[\mathcal{M}], [\mathcal{G}], \mathcal{X}} \quad & \sum_{n=1}^N \sum_{i=3}^N \|\mathbf{M}_{(i)}^{(n,i)}\|_* + \frac{\lambda}{2} \|\mathcal{X} - \Psi([\mathcal{G}])\|_F^2, \\ \text{s.t.} \quad & \mathbf{M}_{(i)}^{(n,i)} = \mathbf{G}_{(i)}^{(n)}, n = 1, \dots, N, i = 1, 2, 3, \\ & P_{\Omega}(\mathcal{X}) = P_{\Omega}(\mathcal{T}), \end{aligned} \quad (12)$$

where $[\mathcal{M}] := \{\mathcal{M}^{(n,i)}\}_{n=1, i=1}^{N,3}$ are the auxiliary variables of $[\mathcal{G}]$. By merging the equal constraints of the auxiliary variables into the Lagrangian equation, the augmented Lagrangian function of TRLRF model is:

$$\begin{aligned} L([\mathcal{G}], \mathcal{X}, [\mathcal{M}], [\mathcal{Y}]) \\ = \sum_{n=1}^N \sum_{i=1}^3 (\|\mathbf{M}_{(i)}^{(n,i)}\|_* + \langle \mathbf{Y}^{(n,i)}, \mathcal{M}^{(n,i)} - \mathcal{G}^{(n)} \rangle \\ + \frac{\mu}{2} \|\mathcal{M}^{(n,i)} - \mathcal{G}^{(n)}\|_F^2) + \frac{\lambda}{2} \|\mathcal{X} - \Psi([\mathcal{G}])\|_F^2, \\ \text{s.t.} \quad P_{\Omega}(\mathcal{X}) = P_{\Omega}(\mathcal{T}), \end{aligned} \quad (13)$$

where $[\mathcal{Y}] := \{\mathbf{Y}^{(n,i)}\}_{n=1, i=1}^{N,3}$ are Lagrangian multipliers, and $\mu > 0$ is a penalty parameter. For $n = 1, \dots, N$, $i = 1, 2, 3$, each $\mathcal{G}^{(n)}$, $\mathcal{M}^{(n,i)}$ and $\mathbf{Y}^{(n,i)}$ is independent, so we can update them by the updating scheme below:

Update $\mathcal{G}^{(n)}$ By using (13), the augmented Lagrangian function w.r.t. $\mathcal{G}^{(n)}$ can be simplified as:

$$\begin{aligned} L(\mathcal{G}^{(n)}) = \sum_{i=1}^3 \frac{\mu}{2} \left\| \mathcal{M}^{(n,i)} - \mathcal{G}^{(n)} + \frac{1}{\mu} \mathbf{Y}^{(n,i)} \right\|_F^2 \\ + \frac{\lambda}{2} \|\mathcal{X} - \Psi([\mathcal{G}])\|_F^2 + C_{\mathcal{G}}, \end{aligned} \quad (14)$$

where the constant $C_{\mathcal{G}}$ consists of other parts of the Lagrangian function which is irrelevant to updating $\mathcal{G}^{(n)}$. This is a least squares problem, so for $n = 1, \dots, N$, $\mathcal{G}^{(n)}$ can be updated by:

$$\begin{aligned} \mathcal{G}^{(n)} = \text{fold}_2 \left(\left(\sum_{i=1}^3 (\mu \mathbf{M}_{(2)}^{(n,i)} + \mathbf{Y}_{(2)}^{(n,i)}) \right. \right. \\ \left. \left. + \lambda \mathbf{X}_{<n>} \mathbf{G}_{<2>}^{(\neq n)} \right) (\lambda \mathbf{G}_{<2>}^{(\neq n),T} \mathbf{G}_{<2>}^{(\neq n)} + 3\mu \mathbf{I})^{-1} \right), \end{aligned} \quad (15)$$

where $\mathbf{I} \in \mathbb{R}^{R_n^2 \times R_n^2}$ denotes the identity matrix.

Update $\mathcal{M}^{(n,i)}$ For $i = 1, 2, 3$, the augmented Lagrangian functions w.r.t. $[\mathcal{M}]$ is conducted by:

$$\begin{aligned} L(\mathcal{M}^{(n,i)}) = \frac{\mu}{2} \left\| \mathcal{M}^{(n,i)} - \mathcal{G}^{(n)} + \frac{1}{\mu} \mathbf{Y}^{(n,i)} \right\|_F^2 \\ + \|\mathbf{M}_{(i)}^{(n,i)}\|_* + C_{\mathcal{M}}. \end{aligned} \quad (16)$$

The above formulation has a closed-form (Cai, Candès, and Shen 2010), which is given by:

$$\mathcal{M}^{(n,i)} = \text{fold}_i \left(D_{\frac{1}{\mu}} \left(\mathbf{G}_{(i)}^{(n)} - \frac{1}{\mu} \mathbf{Y}_{(i)}^{(n,i)} \right) \right), \quad (17)$$

where $D_{\beta}(\cdot)$ is the singular value thresholding (SVT) operation, e.g., if $\mathbf{U}\mathbf{S}\mathbf{V}^T$ is the singular value decomposition of matrix \mathbf{A} , then $D_{\beta}(\mathbf{A}) = \mathbf{U} \max\{\mathbf{S} - \beta \mathbf{I}, 0\} \mathbf{V}^T$.

Update \mathcal{X} The augmented Lagrangian functions w.r.t. \mathcal{X} is:

$$\begin{aligned} L(\mathcal{X}) = \frac{\lambda}{2} \|\mathcal{X} - \Psi([\mathcal{G}])\|_F^2 + C_{\mathcal{X}}, \\ \text{s.t.} \quad P_{\Omega}(\mathcal{X}) = P_{\Omega}(\mathcal{T}), \end{aligned} \quad (18)$$

which is equivalent to tensor decomposition based model in (2). \mathcal{X} is updated by inputting the observed values in the corresponding entries, and approximate the missing entries by updated TR factors $[\mathcal{G}]$ for every iteration, i.e.,

$$\mathcal{X} = P_{\Omega}(\mathcal{T}) + P_{\bar{\Omega}}(\Psi([\mathcal{G}])), \quad (19)$$

where $\bar{\Omega}$ is the set of indices of missing entries which is complement to Ω .

Update $\mathbf{Y}^{(n,i)}$ For $n = 1, \dots, N$ and $i = 1, 2, 3$, the Lagrangian multiplier $\mathbf{Y}^{(n,i)}$ is updated by:

$$\mathbf{Y}^{(n,i)} = \mathbf{Y}^{(n,i)} + \mu (\mathcal{M}^{(n,i)} - \mathcal{G}^{(n)}). \quad (20)$$

In addition, the penalty term of the Lagrangian functions L is restricted by μ which is also updated for every iteration by $\mu = \max\{\rho\mu, \mu_{\max}\}$ and $1 < \rho < 1.5$ is a tuning hyper parameter.

The ADMM based solving scheme is updated iteratively based on the above equations. Moreover, we consider to set two optimization stopping conditions: maximum number of iterations k_{\max} and the difference between two iterations (i.e. $\|\mathcal{X} - \mathcal{X}_{\text{last}}\|_F / \|\mathcal{X}\|_F$) which is thresholded by tolerance tol . The implementation process and hyper-parameter selection of TRLRF is summarized in Algorithm 1. It should be noted that our TRLRF model is non-convex, so the convergence to global minimum can not be theoretically guaranteed. However, the convergence of our algorithm can be verified empirically (see experiment details in Figure 1). Moreover, the extensive experiment results in the next section can also illustrate the stability and effectiveness of TRLRF.

Computational complexity

We analyze the computational complexity of our TRLRF algorithm as follows. If we denote the order of tensor by N , and the TR-rank is set as $R_1 = R_2 = \dots = R_N = R$, for a tensor $\mathcal{X} \in \mathbb{R}^{I_1 \times I_2 \times \dots \times I_N}$, the computational complexity of updating $[\mathcal{M}]$ is mainly cost by SVD operation,

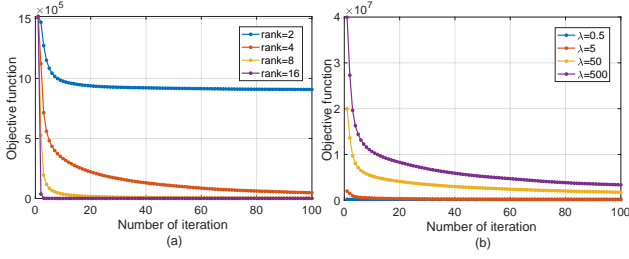


Figure 1: Convergence property illustration of TRLRF under different hyper-parameters. A synthetic tensor with TR structure (size $7 \times 8 \times 7 \times 8$ with TR-rank $\{4, 4, 4, 4\}$, missing rate 0.5) is tested. The experiment records the change of the objective function values by the number of iterations. Each independent experiment is conducted 100 times and the average results are shown in the graphs. (a) and (b) are the convergence curve when TR-rank and λ are changed respectively.

Algorithm 1 Tensor ring low-rank factors (TRLRF)

- 1: **Input:** $P_\Omega(\mathcal{T})$, initial TR-rank $\{R_n\}_{n=1}^N$.
- 2: **Initialization:** For $n = 1, \dots, N, i = 1, 2, 3$, random sample $\mathcal{G}^{(n)}$ by distribution $\mathcal{N} \sim (0, 1)$, $\mathcal{Y}^{(n,i)} = 0$, $\mathcal{M}^{(n,i)} = 0$, $\lambda = 5$, $\mu^0 = 1$, $\mu_{max} = 10^2$, $\rho = 1.01$, $tol = 10^{-6}$, $k = 0$, $k_{max} = 300$.
- 3: **For** $k = 1$ to k_{max} **do**
- 4: $\mathcal{X}_{last} = \mathcal{X}$.
- 5: Update $\{\mathcal{G}^{(n)}\}_{n=1}^N$ by (15).
- 6: Update $\{\mathcal{M}^{(n,i)}\}_{n=1,i=1}^{N,3}$ by (17).
- 7: Update \mathcal{X} by (19).
- 8: Update $\{\mathcal{Y}^{(n,i)}\}_{n=1,i=1}^{N,3}$ by (20).
- 9: $\mu = \max(\rho\mu, \mu_{max})$.
- 6: **If** $\|\mathcal{X} - \mathcal{X}_{last}\|_F / \|\mathcal{X}\|_F < tol$, **break**
- 7: **End for**
- 8: **Output:** completed tensor \mathcal{X} and TR factors $[\mathcal{G}]$.

which is $\mathcal{O}(\sum_{n=1}^N 2I_n R^3 + I_n^2 R^2)$. The computational complexity costed by calculating $\mathcal{G}_{\langle 2 \rangle}^{(\neq n)}$ and updating $[\mathcal{G}]$ are $\mathcal{O}(NR^3 \prod_{i=1, i \neq n}^N I_i)$ and $\mathcal{O}(NR^2 \prod_{i=1}^N I_i + NR^6)$ respectively. If we assume $I_1 = I_2 = \dots = I_N = I$, then overall complexity of our proposed algorithm can be written as $\mathcal{O}(NR^2 I^N + NR^6)$.

Compared to HaLRTC and TRALS which are the representative of the nuclear norm based and the tensor decomposition based algorithms, the computational complexity of HaLRTC is $\mathcal{O}(NI^{N+1})$. TRALS is based on ALS method and TR decomposition, its computational complexity is $\mathcal{O}(PNR^4 I^N + NR^6)$, where P denotes the observation rate. We can see that the computational complexity of our TRLRF is similar to the two related algorithms. However, the characteristic of rank selection robustness of our algorithm can help relieve the work for model selection in practice, thus the computational cost can be reduced. Moreover, though the computational complexity of TRLRF is of

high power in R , due to the high representation ability and flexibility of TR decomposition, the TR-rank is always set as a small value. In addition, from experiments we find out that our algorithm is able to work efficiently in high-order tensors, so we can tensorize the data to a higher-order and choose a small TR-rank to reduce the computational complexity.

Experiment Results

Synthetic data

We first conduct experiments to testify the rank robustness of our algorithm by comparing TRALS, TRWOPT, and our TRLRF. To verifying the performance of the three algorithms, we test two tensors of size $20 \times 20 \times 20 \times 20$ and $7 \times 8 \times 7 \times 8 \times 7 \times 8$. The tensors are generated by TR factors of TR-ranks $\{6, 6, 6, 6\}$ and $\{4, 4, 4, 4, 4, 4\}$ respectively. The values of the TR factors are drawn from *i.i.d.* Gaussian distribution $\mathcal{N} \sim (0, 0.5)$. The observed entries of the tensors are randomly removed by missing rate 0.5, where the missing rate is calculated by $1 - M/\text{num}(\mathcal{T}_{real})$ and M is the number of sampled entries (i.e. observed entries). We record the completion performance of the three algorithms by selecting different TR-ranks. The evaluation index is RSE which is defined by $\text{RSE} = \|\mathcal{T}_{real} - \mathcal{X}\|_F / \|\mathcal{T}_{real}\|_F$, where \mathcal{T}_{real} is the known tensor with full observations and \mathcal{X} is the recovered tensor calculated by each tensor completion algorithm. The hyper-parameters of our TRLRF are set according to Algorithm 1. All the hyper-parameters of TRALS and TRWOPT are set according to the corresponding papers to get the best results.

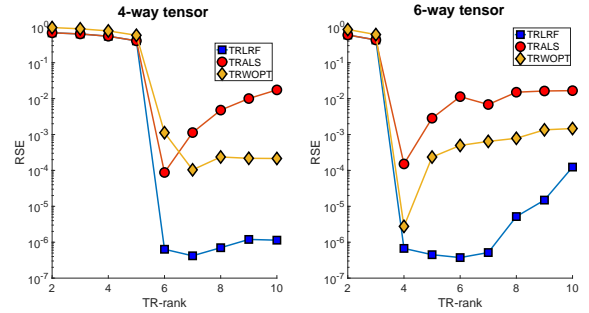


Figure 2: Completion performance of three TR-based algorithms in synthetic data experiment. RSE values of different selected TR-ranks are recorded. The missing rate of the two target tensors is 0.5 and the real TR-ranks are 6 and 4 respectively.

Figure 2 shows the final RSE results which are the average values of 100 times of independent experiments for each case. From the figure we can see, all the three algorithms have their the lowest RSE values when the real TR-ranks of the tensors are chosen and the best performance is obtained from our TRLRF. Moreover, when the TR-rank increases, the performance of TRLRF remains stable while the performance of the other two compared algorithms falls drastically. This indicates that giving low-rankness assump-

tion on TR factors can bring robustness to rank selection, which largely alleviates the model selection problem in the experiments.

Benchmark images inpainting



Figure 3: The eight benchmark images. The first image is named “Lena” and is used in the next two experiments.

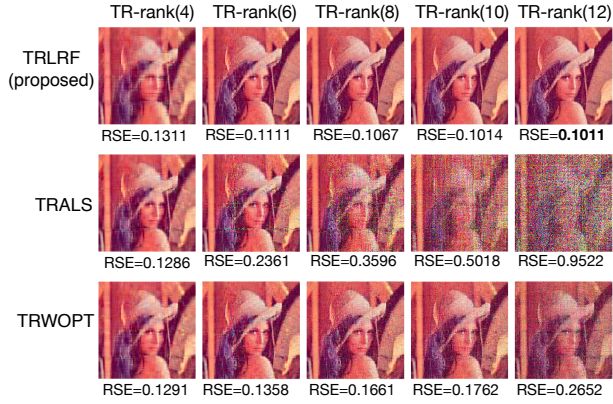


Figure 4: Visual completion results of TRLRF (proposed), TRALS, and TRWOPT on image “Lena” with different TR-ranks when the missing rate is 0.8. The selected TR-ranks are 4, 6, 8, 10, 12 respectively from the first column to the last column. The RSE results are noted under each picture.

In this section, we test our TRLRF and the state-of-the-art algorithms on eight benchmark images which are shown in Figure 3. The size of each RGB image is $256 \times 256 \times 3$ which can be considered as a three-order tensor. For the first experiment, we continue to testify the TR-rank robustness of TRLRF on the image named “Lena”. Figure 4 shows the completion results of TRLRF, TRALS, and TRWOPT when different TR-ranks for each algorithm are selected. The missing rate of the image is set as 0.8, which is the case that the TR decomposition is easy to overfitting. From the figure we can see, our TRLRF gives better results than the other two TR-based algorithms in each case and the highest performance is obtained when TR rank is set as 12. When TR-rank increases, the completion performance of TRALS and TRLRF decreases due to redundant model complexity and overfitting of the algorithms, while our TRLRF shows better results even the selected TR-rank is larger than the desired TR-rank.

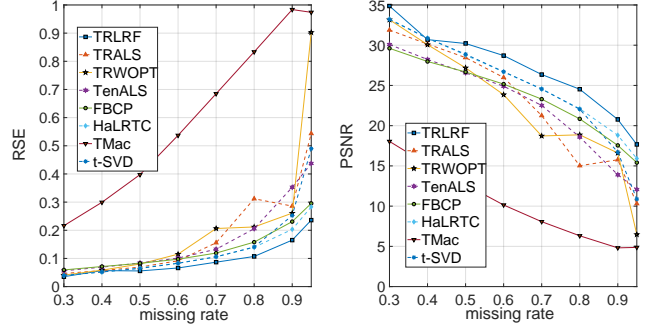


Figure 5: Average completion performance of eight algorithms under different missing rates

In the next experiment, we compare our TRLRF to the two TR-based algorithm TRALS and TRWOPT, and the other state-of-the-art algorithms, i.e., TenALS (Jain and Oh 2014), FBCP (Zhao, Zhang, and Cichocki 2015), HaLRTC (Liu et al. 2013), TMac (Xu et al. 2013) and t-SVD (Zhang et al. 2014). We test these algorithms on all the eight benchmark images by different missing rates: 0.3, 0.4, 0.5, 0.6, 0.7, 0.8, 0.9 and 0.95. Relative square error (RSE) and peak signal-to-noise ratio (PSNR) are adopted for the evaluation of the completion performance. For RGB image data, PSNR is defined as $PSNR = 10 \log_{10}(255^2/MSE)$ where MSE is calculated by $MSE = \|\mathcal{T}_{real} - \mathcal{X}\|_F^2 / \text{num}(\mathcal{T}_{real})$, and $\text{num}(\cdot)$ denotes the number of element of the fully observed tensor.

For the three TR-based algorithms, we assume the TR-ranks are equal for every core tensor (i.e. $R_1 = R_2 = \dots = R_N$). The best completion results for each algorithm are obtained by selecting best TR-ranks for the TR-based algorithms by cross-validation method. Actually finding the best TR-rank to get the best completion results is an annoying work. However, this is much easier for our proposed algorithm because the performance of TRLRF is fairly stable even though the TR-rank is selected in a wide large. For the other five compared algorithms, we tune the hyper-parameters according to the suggestions of each paper to obtain the best completion results. Finally, we show the average performance of the eight images for each algorithm under different missing rates by line graphs. Figure 5 shows the RSE and PSNR results of each algorithm. The smaller RSE value and the larger PSNR value denote the better performance. Our TRLRF performs the best among all the compared algorithms in most cases. When the missing rate increases, the completion results of all the algorithms decrease, especially when the missing rate is near 0.9. The performance of most algorithm falls drastically when the missing rate is 0.95, however, the performance of TRLRF, HaLRTC, and FBCP remains stable and the best performance is obtained from our TRLRF.

Hyperspectral image

A hyperspectral image (HSI) of size $200 \times 200 \times 80$ which records an area of the urban landscape is tested in

Table 1: HSI completion results (RSE) under three different tensor orders with different rank selections

	TRLRF	TRALS	TRWOPT	TMac	TenALS	t-SVD	FBCP	HaLRTC
3-order, high-rank($R_n = 12$)	0.06548	0.07049	0.06695	0.1662	0.3448	0.4223	0.2363	0.1254
3-order, low-rank($R_n = 8$)	0.1166	0.1245	0.1249	0.2963	0.3312	-	-	-
5-order, high-rank($R_n = 22$)	0.1035	0.1392	0.1200	0.8064	-	0.9504	0.3833	0.3944
5-order, low-rank($R_n = 18$)	0.1062	0.1122	0.1072	0.7411	-	-	-	-
8-order, high-rank($R_n = 24$)	0.1190	0.1319	0.1637	0.9487	-	0.9443	0.4021	0.9099
8-order, low-rank($R_n = 20$)	0.1421	0.1581	0.1767	0.9488	-	0.9450	0.4135	0.9097

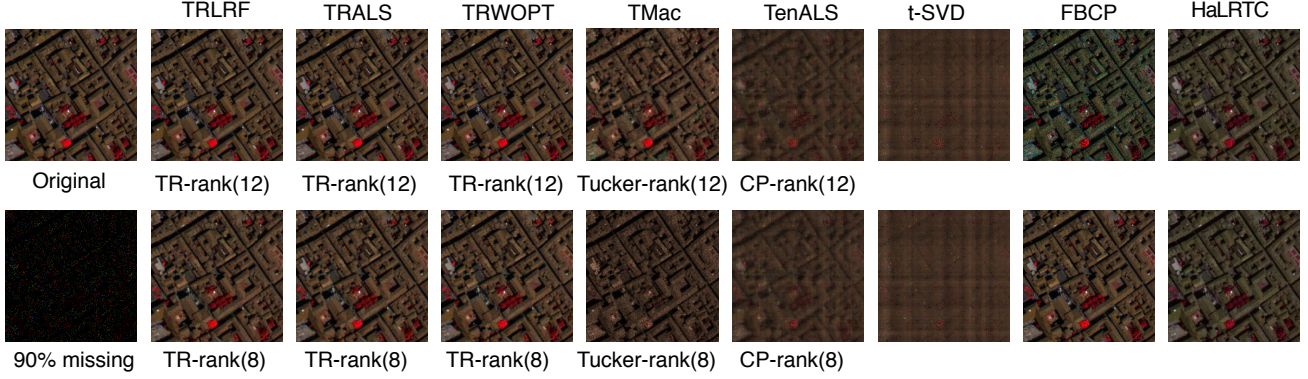


Figure 6: HSI completion results of eight algorithms under 0.9 missing rate. The channels 80, 34, 9 are picked to show the visual results. The rank selection of TRLRF, TRALS, TRWOPT, TMac and TenALS are noted under each according images.

this section¹. In order to test the performance of TRLRF in higher-order tensors, the HSI data is reshaped to higher-order tensors, which is an easy method to find more low-rank features of the data. Moreover, a proper high-order tensorization scheme can reduce the computational complexity of our algorithm. We compare our TRLRF to the other seven tensor completion algorithms in three-order tensor ($200 \times 200 \times 80$), five-order tensor ($10 \times 20 \times 10 \times 20 \times 80$) and eight-order tensor ($8 \times 5 \times 5 \times 8 \times 5 \times 5 \times 8 \times 10$) cases. The higher-order tensor is generated from original HSI data by directly reshaping it to the specified size and order.

The experiment aims to testify the completion performance of the eight algorithms under different model selections, so the experiment variables are the tensor order and tensor rank. The missing rates of all the cases are set as 0.9. All the tuning parameters of each algorithm is set properly according to the statement in the previous experiments. Besides, for the experiments of each order, we choose two different tensor rank: high-rank and low-rank for algorithms which need to set rank manually. It should be noted that the CP-rank of TenALS and the Tucker-rank of TMac are set the same values as TR-rank. The completion performance of RSE results and visual results are listed in Table 1 and Figure 6. The results of FBCP, HaLRTC and t-SVD are not affected by tensor rank, so the cases of the same order with different rank are left blank in Table 1. TenALS cannot deal with tensor more than three-order so the high-order tensor cases for TenALS are also left blank. As shown in Table 1,

our TRLRF gives the best recovery performance for the HSI image. In the three-order cases, the best performance is obtained when TR-rank is 12, however, when the rank is set as 8, the performance of TRLRF, TRALS, TRWOPT, TMac, and TenALS falls because of the underfitting of the selected models. For 5-order cases, when the rank increases from 18 to 22, the performance of TRLRF keeps steady while the performance of TRALS, TRWOPT, and TMac decreases. This is because the high-rank makes the models overfitting and our TRLRF works steadily due to the feature of TR-rank robustness. In eight-order tensor cases, similar properties can be obtained and our TRLRF also performs the best.

Conclusion

In this paper, we propose an efficient and high-performance tensor completion algorithm based on TR decomposition, which introduces low-rank constraints on the TR latent space. The model imposes low-rank surrogates on tensor latent factors and minimizes the approximation error of the observed tensor and the recovered tensor. The model is efficiently solved by ADMM algorithm and it can effectively deal with model selection which is a common problem in most traditional tensor completion methods, thus providing much less computational cost. The extensive experiments in various situations by synthetic data and real-world data show that our algorithm outperforms the state-of-the-art algorithms. Furthermore, the proposed method can be extended to various tensor decompositions to develop more efficient and robust algorithms.

¹http://www.ehu.eus/ccwintco/index.php/Hyperspectral_Remote_Sensing_Scenes

References

- [Acar et al. 2011] Acar, E.; Dunlavy, D. M.; Kolda, T. G.; and Mørup, M. 2011. Scalable tensor factorizations for incomplete data. *Chemometrics and Intelligent Laboratory Systems* 106(1):41–56.
- [Anandkumar et al. 2014] Anandkumar, A.; Ge, R.; Hsu, D.; Kakade, S. M.; and Telgarsky, M. 2014. Tensor decompositions for learning latent variable models. *The Journal of Machine Learning Research* 15(1):2773–2832.
- [Boyd et al. 2011] Boyd, S.; Parikh, N.; Chu, E.; Peleato, B.; Eckstein, J.; et al. 2011. Distributed optimization and statistical learning via the alternating direction method of multipliers. *Foundations and Trends® in Machine learning* 3(1):1–122.
- [Cai, Candès, and Shen 2010] Cai, J.-F.; Candès, E. J.; and Shen, Z. 2010. A singular value thresholding algorithm for matrix completion. *SIAM Journal on Optimization* 20(4):1956–1982.
- [Cong et al. 2015] Cong, F.; Lin, Q.-H.; Kuang, L.-D.; Gong, X.-F.; Astikainen, P.; and Ristaniemi, T. 2015. Tensor decomposition of EEG signals: a brief review. *Journal of Neuroscience Methods* 248:59–69.
- [Filipović and Jukić 2015] Filipović, M., and Jukić, A. 2015. Tucker factorization with missing data with application to low- n n -rank tensor completion. *Multidimensional systems and signal processing* 26(3):677–692.
- [Gandy, Recht, and Yamada 2011] Gandy, S.; Recht, B.; and Yamada, I. 2011. Tensor completion and low- n -rank tensor recovery via convex optimization. *Inverse Problems* 27(2):025010.
- [Grasedyck, Kluge, and Kramer 2015] Grasedyck, L.; Kluge, M.; and Kramer, S. 2015. Variants of alternating least squares tensor completion in the tensor train format. *SIAM Journal on Scientific Computing* 37(5):A2424–A2450.
- [Hillar and Lim 2013] Hillar, C. J., and Lim, L.-H. 2013. Most tensor problems are NP-hard. *Journal of the ACM (JACM)* 60(6):45.
- [Imaizumi, Maehara, and Hayashi 2017] Imaizumi, M.; Maehara, T.; and Hayashi, K. 2017. On tensor train rank minimization: Statistical efficiency and scalable algorithm. In *Advances in Neural Information Processing Systems*, 3933–3942.
- [Jain and Oh 2014] Jain, P., and Oh, S. 2014. Provable tensor factorization with missing data. In *Advances in Neural Information Processing Systems*, 1431–1439.
- [Kanagawa et al. 2016] Kanagawa, H.; Suzuki, T.; Kobayashi, H.; Shimizu, N.; and Tagami, Y. 2016. Gaussian process nonparametric tensor estimator and its minimax optimality. In *International Conference on Machine Learning*, 1632–1641.
- [Kolda and Bader 2009] Kolda, T. G., and Bader, B. W. 2009. Tensor decompositions and applications. *SIAM review* 51(3):455–500.
- [Liu et al. 2013] Liu, J.; Musialski, P.; Wonka, P.; and Ye, J. 2013. Tensor completion for estimating missing values in visual data. *IEEE transactions on pattern analysis and machine intelligence* 35(1):208–220.
- [Liu et al. 2014] Liu, Y.; Shang, F.; Fan, W.; Cheng, J.; and Cheng, H. 2014. Generalized higher-order orthogonal iteration for tensor decomposition and completion. In *Advances in Neural Information Processing Systems*, 1763–1771.
- [Liu et al. 2015] Liu, Y.; Shang, F.; Jiao, L.; Cheng, J.; and Cheng, H. 2015. Trace norm regularized candecomp/parafac decomposition with missing data. *IEEE transactions on cybernetics* 45(11):2437–2448.
- [Novikov et al. 2015] Novikov, A.; Podoprikin, D.; Osokin, A.; and Vetrov, D. P. 2015. Tensorizing neural networks. In *Advances in Neural Information Processing Systems*, 442–450.
- [Oseledets 2011] Oseledets, I. V. 2011. Tensor-train decomposition. *SIAM Journal on Scientific Computing* 33(5):2295–2317.
- [Signoretto et al. 2014] Signoretto, M.; Dinh, Q. T.; De Lathauwer, L.; and Suykens, J. A. 2014. Learning with tensors: a framework based on convex optimization and spectral regularization. *Machine Learning* 94(3):303–351.
- [Wang, Aggarwal, and Aeron 2017] Wang, W.; Aggarwal, V.; and Aeron, S. 2017. Efficient low rank tensor ring completion. *Rn* 1(r1):1.
- [Xu et al. 2013] Xu, Y.; Hao, R.; Yin, W.; and Su, Z. 2013. Parallel matrix factorization for low-rank tensor completion. *arXiv preprint arXiv:1312.1254*.
- [Yuan, Zhao, and Cao 2017] Yuan, L.; Zhao, Q.; and Cao, J. 2017. Completion of high order tensor data with missing entries via tensor-train decomposition. In *International Conference on Neural Information Processing*, 222–229. Springer.
- [Zhang et al. 2014] Zhang, Z.; Ely, G.; Aeron, S.; Hao, N.; and Kilmer, M. 2014. Novel methods for multilinear data completion and de-noising based on tensor-svd. In *Proceedings of the IEEE Conference on Computer Vision and Pattern Recognition*, 3842–3849.
- [Zhao et al. 2016a] Zhao, Q.; Zhou, G.; Xie, S.; Zhang, L.; and Cichocki, A. 2016a. Tensor ring decomposition. *arXiv preprint arXiv:1606.05535*.
- [Zhao et al. 2016b] Zhao, Q.; Zhou, G.; Zhang, L.; Cichocki, A.; and Amari, S.-I. 2016b. Bayesian robust tensor factorization for incomplete multiway data. *IEEE transactions on neural networks and learning systems* 27(4):736–748.
- [Zhao et al. 2018] Zhao, Q.; Sugiyama, M.; Yuan, L.; and Cichocki, A. 2018. Learning efficient tensor representations with ring structure networks.
- [Zhao, Zhang, and Cichocki 2015] Zhao, Q.; Zhang, L.; and Cichocki, A. 2015. Bayesian cp factorization of incomplete tensors with automatic rank determination. *IEEE transactions on pattern analysis and machine intelligence* 37(9):1751–1763.